IOP Conference Series: Materials Science and Engineering

PAPER • **OPEN ACCESS**

Thermal behaviour and microstructural analysis of Sn-40Pb alloy and Sn-40Pb soldered on electroless nickel/immersion gold

To cite this article: Ai Ling Teoh *et al* 2020 *IOP Conf. Ser.: Mater. Sci. Eng.* **957** 012061

IOP Conf. Series: Materials Science and Engineering **957** (2020) 012061 doi:10.1088/1757-899X/957/1/012061

Thermal behaviour and microstructural analysis of Sn-40Pb alloy and Sn-40Pb soldered on electroless nickel/immersion gold

Ai Ling Teoh[1,*], *Mohd Arif Anuar* Mohd Salleh[1] , *Dewi Suriyani* Che Halin[1] , and *Kai Loong* Foo[2]

[1]School of Materials Engineering, Universiti Malaysia Perlis (UniMAP), Taman Muhibbah, 02600 Jejawi, Arau, Perlis, Malaysia
[2]Nano Biochip Research Group, Institute of Nano Electronic Engineering (INEE), Universiti Malaysia Perlis (UniMAP), 01000 Kangar, Perlis, Malaysia

Abstract. Due to the toxicity of lead solder, the lead-free solder has been developing and improved in order to replace the lead solder. However, the behaviour and properties of lead solder is still better than the lead-free solder, especially in application when soldering on substrate. Hence, a common lead solder, Sn-40Pb is studied in this research by comparing with Sn-40Pb soldering on electroless nickel/immersion gold (ENIG) substrate. The thermal behaviour by differential scanning calorimeter (DSC) and microstructure formation with elemental analysis by scanning electron microscope (SEM) were carried out for Sn-40Pb solder alloy and Sn-40Pb soldered on ENIG substrate in this study. The result showed that the pasty range of Sn-40Pb was lower than Sn-40Pb/ENIG while the undercooling was higher. The diffusion and dissolution of Ni and Cu elements from ENIG substrate into the solder, forming the lead-rich phase with Ni elements and interfacial $(Cu,Ni)_6Sn_5$ with Pb elements in Sn-40Pb/ENIG. The diffusion and dissolution of elements from substrate into the solder affects the thermal behaviour and microstructural of solder.

1 Introduction

Due to the legislation by the Waste of Electrical and Electronic Equipment (WEEE) and the directives on the restriction of hazardous substance (RoHS), the lead-free solders that is green and friendly to the environment is focused for developing since lead solder is a toxic material which is harmful to human health and also the environment. However, the lead solder is still having better eutectic composition properties which are good in mechanical properties, good wettability, low cost and low melting point. Hence, the further understanding of lead solder is important for enhancing the properties of lead-free solder [1-4].

As different formation of microstructure resulted in various solder joint properties mechanically which causes different reliability of electronic devices, the thermal behaviour of solder plays a main role for application. Chu et al. has compared and studied the thermal

* Corresponding author: akirateoh@gmail.com

analysis by differential scanning calorimeter method and microstructures for different composition of tin-lead solders in past [5]. On the other hand, Cruz et al. has carried out the thermal analysis for different composition of tin-lead solders by cooling curve method [6].

Solder is always used for the bonding and interconnect purpose in application, and hence it is direct contacting the substrate in electronic devices during soldering process. The degree of undercooling during solidification for solder on substrate affects the solder joint's microstructure forming which resulted in different electronic device's performance. However, most of the researches were focused on the thermal analysis of solder itself or soldering above the substrate of copper. Hence, the aim of this research is to understand the effects of ENIG substrate to the Sn-40Pb solder through the behaviour of thermal and its changing on microstructures.

2 Experimental Procedures

2.1 Sample preparation

The Sn-40Pb solder alloy was melted at 350 °C for 1 hour in the electric resistance furnace and then poured into the mould of stainless-steel for casting. Some casted metal sheets were rolled into the thickness of 50 µm as metal foils and next punched into round shape with 3 mm diameter puncher, while other metal sheets were kept for the solder analysis. After applying the rosin mildly activated (RMA) flux onto the 3 mm punched metal foil, it was then put on the Pyrex sheet and reflowed in the oven forming sphere shape as the 900 µm solder ball due to the surface tension effect. Next, some solder balls were reflowed on the ENIG substrate once the RMA flux was applied, while other solder balls were kept for another testing.

2.2 Thermal analysis

The differential scanning calorimeter (DSC) model Q10 was used to analyse the solder's thermal behaviour of 5 mg of Sn-40Pb metal sheet. To understand the Sn-40Pb/ENIG behaviour of thermal, the RMA flux was applied on the 3.2 mg solder ball and then this solder ball was put on the ENIG substrate. By using the rate of 10 °C/min, heating up both test samples to 270 °C and then following by cooling down to 30 °C inside the inert nitrogen gas chamber to obtain the exothermic and endothermic curves for thermal analysis.

2.3 Microstructural analysis

Scanning electron microscope (SEM) model JEOL JSM 6460LA equipped with Energy Dispersive X-ray (EDX) was used to observe the microstructure and analyse the element of Sn-40Pb solder and the Sn-40Pb/ENIG after sample grinding, polishing and etching.

3 Result and Discussions

3.1 Thermal behaviour

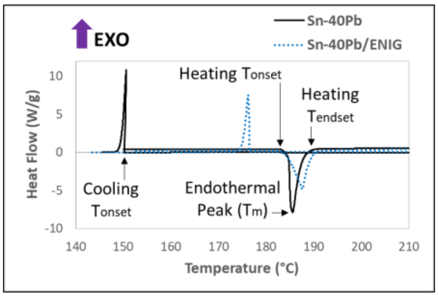

Fig. 1. Heating (endothermal) and cooling (exothermal) DSC results of Sn-40Pb and Sn-40Pb /ENIG.

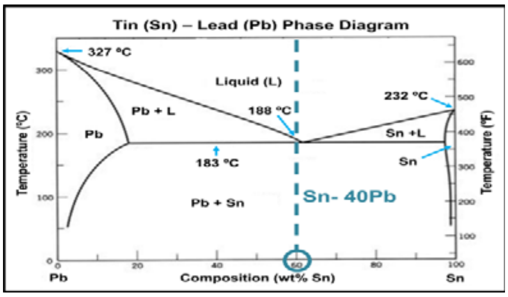

Fig. 2. The Sn-Pb equilibrium phase diagram [7].

In order to obtain a good performance of electronic device, the solder joint properties need to be studied and understood through the solder characterization of cooling and melting. To mimic the ball-grid array (BGA) application [8], DSC analysis was carried out to study the samples' thermal behaviour at 10 °C/min of cooling and heating rate. Fig. 1, Table 1 and Table 2 show the results of DSC. Both thermal behaviour of Sn-40Pb solder and Sn-40Pb/ENIG were tested and analysed. The heating, T_{onset} of Sn-40Pb and Sn-40Pb/ENIG where the endothermic reaction during heating up was begun at 184.71 and 182.76 °C respectively. The heating result plot is then achieving the peaks at 185.57 and 187.57 °C for Sn-40Pb and Sn-40Pb/ENIG respectively and labelled as Tm. Fig. 2 displays the Sn-Pb binary phase diagram. Based on the equilibrium phase diagram for Sn-Pb, the phase changing of (Pb+Sn) into the phase of (Pb+L) was occurred at the temperature of 183 °C which is the T_{onset}. Accordingly to the research by Cho et al., it has showed that the findings are similar to above DSC results [9].

On top of that, El-Daly et al. and Sayyadi et al. have reported that the pasty range is one of the thermal behaviour of material and can be formulated as:

$$\text{Pasty range} = \text{Heating } T_{endset} - \text{Heating } T_{onset} \tag{1}$$

where heating T_{onset} is the solidus temperature and T_{endset} is the liquidus temperature during heating [8, 10]. By calculation, Table 1 displays the pasty range of Sn-40Pb and Sn-40Pb/ENIG respectively 6.80 and 10.01 °C. With the existing of heat, soldering process has been taking part between the solder and substrate causing an increasing of pasty range of Sn-40Pb/ENIG, compared to Sn-40Pb solder itself. Furthermore, the degree of undercooling is another important parameter that affects the reliability of solder joint which determines the solder solidification behaviour ; and this parameter can be obtained from the DSC curve. Elmer et al. and Kang et al. have defined the undercooling as the deduction of heating T_{onset}, which is the starting point of melting in heating curve; to cooling T_{onset}, which is the starting point of solidification in cooling curve [11, 12]; and it can be formulated as:

$$\text{Undercooling, } \Delta T = \text{Heating } T_{onset} - \text{Cooling } T_{onset} \tag{2}$$

The undercooling degree of Sn-40Pb and Sn-40Pb/ENIG is 34.43 and 6.25 °C respectively ; showing that with the existing of substrate, the undercooling degree for Sn-40Pb/ENIG is decreasing compared to Sn-40Pb. Cho et al. has been reported the similar results where the tin-rich solder alloys have lower undercooling when the solder reacts with the substrate. The wettable surface of substrate facilitates the reaction between both substrate and solder during the solidification [9]. In this research, the substrate with ENIG surface finish has given a wettable surface to the Sn-40Pb solder during the soldering process; enabling the substrate elements for example Ni to diffuse and dissolve into the solder during solidification, resulted in the decreasing of undercooling degree.

Table 1. Heating peak (T_m), solidus temperature (heating T_{onset}), liquidus temperature (heating T_{endset}) and pasty range for Sn-40Pb and Sn-40Pb/ENIG.

Sample	Heating Peak T_m (°C)	Heating T_{onset} (°C)	Heating T_{endset} (°C)	Pasty Range $T_{onset} - T_{endset}$ (°C)
Sn-40Pb	185.57	184.71	191.51	6.80
Sn-40Pb/ENIG	187.57	182.76	192.77	10.01

Table 2. Starting point of solidification (cooling T_{onset}) and degree of undercooling (ΔT) for Sn-40Pb and Sn-40Pb/ENIG.

Sample	Cooling T_{onset} (°C)	Undercooling ΔT (°C)
Sn-40Pb	150.28	34.43
Sn-40Pb/ENIG	176.50	6.25

3.2 Microstructure observation

Fig. 3 shows the SEM image of Sn-40Pb solder alloy, where it consists of the primary lead-rich phase and secondary tin-rich phase. The research by Cruz et al. has stated that the Sn-12Pb, Sn-22.5Pb and Sn-28.5Pb formed the primary lead-rich phase and secondary tin-rich phase after the solders were solidified [6].

Fig. 4 displays no significant difference of the Sn-40Pb solder microstructure when it is soldered on a substrate, except an interfacial layer was formed between the solder and substrate. The formation of crystals in white color and its grey color matrix in Fig. 4 shows the similar structures as in Fig. 3. EDX analysis was done to study the element formed in the microstructure, especially the interfacial layer between the substrate and solder.

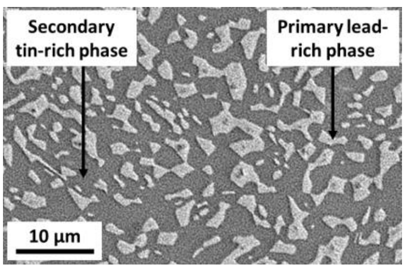

Fig. 3. SEM image of Sn-40Pb solder alloy.

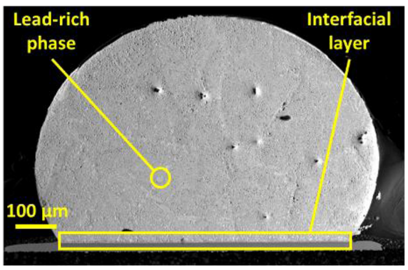

Fig. 4. SEM image of Sn-40Pb soldered on ENIG substrate

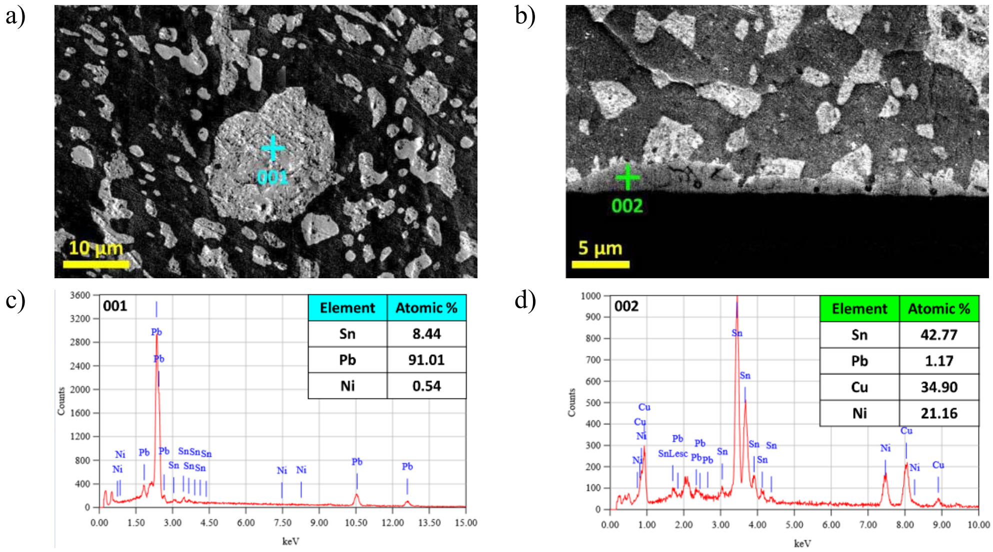

Fig. 5. SEM images and EDX results of Sn-40Pb soldered on ENIG substrate. (a) Lead-rich phase (b) Interfacial layer (c) EDX on lead-rich phase (d) EDX on interfacial layer.

From the EDX result of the lead-rich phase (Fig. 5a) inside the solder ball in Fig. 5c, the phase is having the elements of Sn, Pb, Ni; showing the atomic percentage that forming the highest quantity of lead. Chu et al. has reported in the research that Sn-Pb composition with more than 25 weight percent of lead consists of two nucleation phases which are the primary lead-rich phase and the secondary tin-rich phase as the matrix [5]. On the other hand, Cho et al. has found in the study that the Ni elements are diffused and dissolved from the substrate into the solder during the interfacial reaction when heat is applied [9]. Thus, the crystal nucleated in the solder ball after soldering in Fig. 5a is the lead-rich phase with Ni element since the elements from substrate have diffused and dissolved into the solder.

Moreover, at the contacting area of substrate and solder, there is a growing of a crystal layer as illustrated in Fig. 5b. The forming of this crystal layer is because of the interfacial reaction between the substrate and solder during soldering process. According to the EDX result in Fig. 5d, it exhibits that the interfacial crystals are formed by the Sn, Pb, Cu and Ni elements. Based on the atomic percentage results, the interfacial crystal layer formed was the interfacial intermetallic compound of $(Cu,Ni)_6Sn_5$ with a little amount of Pb element. Salleh et al. has reported the similar intermetallic compound formation of $(Cu,Ni)_6Sn_5$ when Ni element is added into the Sn-0.7Cu alloy [13]. Cu and Ni elements are originated from the substrate where both elements are diffused and dissolved into the solder with the existing of heat during the interfacial reactions [9]. The existence of other elements in the solder caused the decreasing of the undercooling degree since the nucleation of intermetallic compound was begun during solidification process [14-18].

4 Conclusion

The diffusion and dissolution of Ni and Cu elements from ENIG substrate into the solder during solidification resulted in higher pasty range for Sn-40Pb/ENIG compared Sn-40Pb while it reduced the undercooling degree. Both microstructures of Sn-40Pb and Sn-40Pb/ENIG consisted of the primary lead-rich phase and the secondary tin-rich phase.

However, Ni elements dissolved in the lead-rich phase of Sn-40Pb/ENIG while there is no Ni elements in Sn-40Pb solder itself. Furthermore, a layer of intermetallic compound of $(Cu,Ni)_6Sn_5$ with a little amount of Pb element was formed at the interfacial between the substrate and solder.

It is thankfully to the research supporter, Nihon Superior and; the support of materials and financial from an Institutional Links grant, ID 332397914, under the Newton-Ungku Omar Fund partnership. The grant is funded by the UK Department of Business, Energy and Industrial Strategy (BEIS) and Malaysia and delivered by the British Council. It is to acknowledge School of Materials Engineering from Universiti Malaysia Perlis (UniMAP) for the facilities supporting too.

References

1. W.-T. Chen, C. Ho, and C. Kao, J. Mater. Res. **17,** 263-266 (2002)
2. A. El-Daly, A. El-Taher, and S. Gouda, Mater. Des. **65**,796-805 (2015)
3. M. Fazal, N. Liyana, S. Rubaiee, and A. Anas, Measurement (2018)
4. H. A. Jaffery, M. F. M. Sabri, S. M. Said, S. W. Hasan, I. H. Sajid, N. I. M. Nordin, M. M. I. M. Hasnan, D. A. Shnawah, and C. V. Moorthy, J. Alloys Compd. 151925 (2019)
5. M. Chu, Y. Shiohara, and M. C. Flemings, Metall Trans. A **15**, 1303-1310 (1984)
6. H. Cruz, C. Gonzalez, A. Juárez, M. Herrera, and J. Juarez, J. Mater. Process. Technol.**178**, 128-134 (2006)
7. S. Xu, A. H. Habib, A. D. Pickel, and M. E. McHenry, Prog. Mater. Sci. **67**,95-160 (2015)
8. A. El-Daly, W. Desoky, A. Saad, N. Mansor, E. Lotfy, H. Abd-Elmoniem, and H. Hashem Mater. Des. **80**, 152-162 (2015)
9. M. G. Cho, S. K. Kang, and H. M. Lee, J. Mater. Res. **23**, 1147-1154 (2008)
10. R. Sayyadi and H. Naffakh-Moosavy, Mater. Sci. Eng. A **735**, 367-377 (2018)
11. J. W. Elmer, E. D. Specht, and M. Kumar, J. Electron. Mater.**39**, 273-282 (2010)
12. S. K. Kang, M. G. Cho, P. Lauro, and D.-Y. Shih, in 2007 Proceedings 57th Electronic Components and Technology Conference,1597-1603 (2007).
13. M. M. Salleh, S. McDonald, C. Gourlay, S. Belyakov, H. Yasuda, and K. Nogita, J. Electron. Mater. **45**, 154-163 (2016)
14. T. Lu, D. Yi, H. Wang, X. Tu, and B. Wang, J. Alloys. Compd **781**, 633-643 (2019)
15. H. Shang, Z. Ma, S. Belyakov, and C. Gourlay, J. Alloys Compd **715**, 471-485 (2017)
16. X. Tu, D. Yi, J. Wu, and B. Wang, J. Alloys Compd **698**, 317-328 (2017)
17. R. M. Said, M. A.A. M. Salleh, M. N. Derman, M.I.I. Ramli Key Eng. Mater. **700,** 123-131 (2016)
18. M.I.I Ramli, N. Saud, M.A.A Mohd Salleh, M. Nazree Derman, R.Mohd Said, Mater. Sci.Forum 803, 228-232 (2015)